Proceedings of the the Tenth Symposium of Magnetic Measurements, Warsaw, 17–19.10.2011

Effect of Interstitial Iron Defect and Doping on Physical Properties and Stability of Iron Telluride

R. Viennois*

Institut Charles Gerhardt, University Montpellier 2 and CNRS, Pl. E. Bataillon, Montpellier, France
and Condensed Matter Physics Department, University of Geneva, 21 Quai E. Ansermet, Geneva, Switzerland

We report on the effect of interstitial iron defect and doping on iron physical properties and stability of iron telluride by combined experimental and theoretical study. We find that antimony doping and increase iron content in interstitial effect have both the effect to slightly decrease the temperature of the magneto-structural transition T_{trans}. From stability calculations and absence of change in lattice parameters, it is suggested that insertion of antimony did not occur. Large decrease of T_{trans} down to 32 K was observed with Ni doping and our stability calculations confirm that the Ni doping is most favorable in the stability point of view. First-Principles calculations of stability of defect using supercell technique for stoichiometric FeTe indicate that the most stable defect is iron interstitial defect, by far, confirming the proposal done in the literature. Our electronic calculations indicate the appearance of large peaks around the Fermi level in the case of this defect and not just simple doping effect.

PACS: 61.72.–y, 71.55.Ak, 74.70.Xa, 71.20Lp

1. Introduction

In 2008, Hosono and coworkers found new class of high-T_{C} superconductors containing FeAs layers [1]. Therefore, there is a renewal of superconductivity research since this time with the hope to find new high-T_{C} superconducting material classes. Among these new iron based compounds, iron chalcogenide is the simplest because it contains only one type of layer and can help to improve our understanding of the superconducting mechanism whose the origin is thought to be mainly due to spin fluctuations [1, 2]. The absence of charge transfer in the superconducting layer, the presence of iron in interstitial site with square pyramid symmetry and the magnetic ground state of bicollinear type instead of collinear type like in pnictogenide iron based families are the other remarkable peculiarities of these iron chalcogenides. Notably, when alloying the $Fe_{1+x}Te$ compound with Se, the iron content in the interstitial site, x, is a factor crucial for the development or absence of superconductivity in the iron chalcogenides. Indeed, when the amount of iron, x, is too high ($x \geq 0.05$), the superconductivity is suppressed for Se content, $y < 0.45$. For all iron content, no superconductivity is observed when $y < 0.2$ [2, 3]. Actually, only few experimental studies have focused about doping of iron telluride on both sites and there is no theoretical study on the thermodynamic stability of doped compounds and about defects in iron telluride. As the nature of the magnetic ground state of iron telluride is depending of the iron content in the interstitial site, study of the stability and electronic properties of this interstitial defect is of high interest. Moreover, our study of the change of magnetic properties of iron telluride with doping and of the thermodynamic stability of these doped compounds is important for understanding why superconductivity does not occur and if this is related to structural properties. This is the aim of the present paper.

2. Experimental

The undoped samples studied are single-crystalline $Fe_{1+x}Te$ with two different iron contents (nominal starting compositions $x = 0$ and $x = 0.1$ give respectively $x = 0.08$ and $x = 0.13$, as determined by refinement on single-crystal X-ray diffraction experiments) grown by modified Bridgman method [3]. Using the same method for doping iron telluride with 5% of Ni on Fe site and 5% of Sb on Te site gives only polycrystalline bulk samples. An attempt to make 5% of Co doping on Fe site was unsuccessful as Co based secondary phases precipatate. We note that in the two first cases, if we do not see secondary phases by X-ray diffraction, the lattice parameter almost does not change, indicating that the real substitution must be less than the nominal starting 5% content. Magnetic properties were measured using a MPMS Squid magnetometer from Quantum Design. Below and above the magneto-structural transition temperature, we observe perfect linear behavior of the magnetization with the magnetic field, indicating the absence of magnetic impurities in the samples studied in the present paper.

3. Theoretical

First-principles calculations are performed by using the scalar relativistic all-electron Blöchl's projector augmented-wave (PAW) method within the generalized gradient approximation (GGA), as implemented in the highly-efficient Vienna Ab initio Simulation Package (VASP) [4–6]. For the GGA exchange-correlation

* e-mail: Romain.Viennois@univ-montp2.fr

function, the Perdew–Berke–Erzenhof parametrization (PBE) [7] employed for the calculations of the solid solutions with plane-wave energy cutoff of 350 eV. The total energy is converged numerically to less than 1×10^{-5} eV/unit using the Methfessel–Paxton technique and Monkhorst–Pack k-point meshes [8, 9] with a smearing parameter of 0.2 eV and a k-point sampling of $5 \times 5 \times 5$ in a $2 \times 2 \times 2$ supercell containing 32 atoms for doped compounds and antisite defects, 31 atomes for vacancy defects and 33 atoms for the interstitial defect. In the case of doping, one Te atom is replaced by an Sb atom or one Fe atom is replaced by a Co or Ni atom. The interstitial atom is added at the position found experimentally and thus its position is fully relaxed first and thus together with the volume. Calculations done for larger $3 \times 3 \times 2$ supercells for the most stable defect confirm the values found for $2 \times 2 \times 2$ supercell and that the interstitial defect is by far the most stable defect, as it will be seen later. The electronic structure is calculated using Tetrahedron technique as integration method in order to determine the effect of the interstitial defect and dopants on the electronic structure.

4. Results and discussion

In Fig. 1, we report the magnetic susceptibility for pure single-crystalline $Fe_{1+x}Te$ and for doped samples with nominal composition $Fe_{0.95}Ni_{0.05}Te$ and $FeTe_{0.95}Sb_{0.05}$. One can see in every samples strong change in the magnetic susceptibility at low temperature that corresponds to the magneto-structural transition observed in pure Tellurium compounds by using neutron diffraction experiments in several previous works [2, 10]. The observation of a decrease of the magneto-structural transition temperature when increasing the iron content in interstital position agrees with previous observations [10], while Sb and Ni doping decreased the $T_{\rm trans}$ transition temperature too. However, as noted in Table I, if the effective magnetic moment is increasing for the case of Sb doped and $Fe_{1.13}Te$ compared to $Fe_{1.08}Te$, the inverse change is observed for the Ni-doping. We note that the Curie–Weiss follow the inverse tendency than the effective moment and that the change is deconnected with the change of the magnetostructural transition temperature, $T_{\rm trans}$. This could suggest that Curie–Weiss behaviour that occurs in the same temperature range than the negative slope of the resistivity could be due to some Kondo effect [3, 11].

For better understanding the change in the electronic and magnetic properties of pure and doped iron telluride and its thermodynamic stability, structure relaxation and band structure calculations have been done. The issue of the thermodynamic stability has been neglected in the recent works on iron chalcogenides, although it is obvious from an observation of both chemical binary phase diagram of iron–chalcogen atom [12, 13] and of the full magnetic and superconducting phase diagram of these compounds [2, 3, 10] that any change of the ratio Fe/Te

TABLE I

Effective moment, Curie–Weiss temperature, magnetostructural, transition temperature and temperature range of validity of Curie–Weiss law (RR) of the samples.

Composition sample	μ_{eff} [μ_B/f.u.]	$\theta_{\rm CW}$ [K]	$T_{\rm trans}$ [K]	RR [K]
$Fe_{1.08}Te$	3.7	−190	66	150–300
$Fe_{1.13}Te$	3.81	−150	58	145–300
$FeTe_{0.95}Sb_{0.05}$	3.95	−170	56	120–300
$Fe_{0.95}Ni_{0.05}Te$	3.45	−242	32	100–300

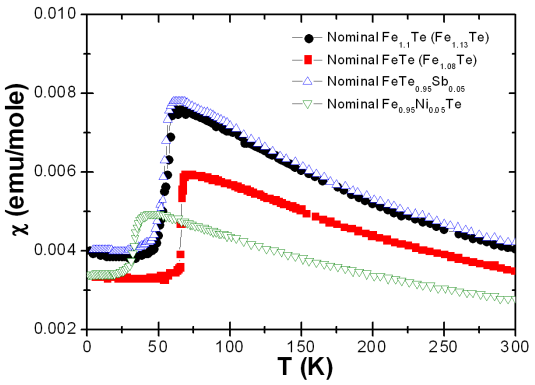

Fig. 1. Thermal variation of the magnetic susceptibility, χ, of the two $Fe_{1+x}Te$ samples with two different 1+x iron content and of 5% Ni and 5% Sb doped samples.

would change the physical properties of these compounds and that the stability domain of these compounds is relatively broad. Notably, pure FeTe is excluded from the known phase diagram and only insertion of iron in interstitial position seems to stabilize the iron telluride phase [12]. Therefore, now, using first principles calculations, we examine several issues concerning the stability of iron telluride and its related compounds and notably what is the most stable defect in that compound, then we will examine the effect of doping on the stability of $Fe_{1+x}Te$ and finally we will examine the impact of interstitial iron atoms and of the dopants on the electronic structure at the vicinity of the Fermi level.

In the present work, we have used the $2 \times 2 \times 2$ supercell for several reasons. Firstly, this makes faster the calculations, but we have also checked that the most stable defects are still the same using larger $3 \times 3 \times 2$ supercell. Secondly, the concentrations of interstial iron atoms and of dopants are closer to the experimental values. In Table II, we report the formation energy of the different cases examined in the present study. As can be seen, we observe that the formation energy in all compounds is slightly positive. Generally speaking, formation energy calculations based on PBE exchange correlation functional are known to underestimate the formation

energy [14] but it predicts formation energy qualitatively correct, so we can make some comparisons. This small positive formation energy indicates that iron telluride is weakly stable compound, notably the stoichiometric one, agreeing with the absence of stable iron telluride close to the Fe/Te = 1 ratio in the phase diagram [12]. Let us now examine the case of the defects in FeTe. We find that the most stable defect is I^{Fe} interstial defect with an energy of 1.13 eV/defect (1.15 eV/defect with the $3 \times 3 \times 2$ supercell), while the other stable defects are much less stable with 1.86 eV/defect (1.76 eV/defect with the $3 \times 3 \times 2$ supercell) in the case of Te^{Fe} antisite defect, 3.49 eV/defect for the case of V^{Te} vacancies (3.19 eV/defect with the $3 \times 3 \times 2$ supercell) and 3.66 eV/defect in the case of Fe^{Te} antisite defect (3.7 eV/defect with the $3 \times 3 \times 2$ supercell). The other defects are even much less stable in FeTe. Therefore, our stability calculations, together with the observed ratio Fe/Te superior to one, confirm that the FeTe contains an excess of iron that is incorporated in interstitial site. Previously, this picture of iron on interstitial site was only proposed based on the results from Rietveld refinement of diffraction pattern in the case of pure iron telluride [2, 3, 10]. However, this issue is not trivial because after thinking first that the off-stoechiometry in iron selenide has the same origin, recent experimental works indicate that the most stable defect in $Fe_{1+x}Se$ is V^{Se} defect and not I^{Fe} defect [15]. Note the relatively good agreement between the calculated z coordinate of the interstitial iron site (see Table II) with the experimental determination ($z_{\mathrm{Feint}} = 0.718$) [3]. Therefore, our present result confirming that the I^{Fe} defect is the most stable defect in $Fe_{1+x}Te$ is an important result for clarifying the situation in the understanding of the defects in the iron chalcogenide compounds.

TABLE II

Calculated crystallographic parameters and formation energies of pure and doped iron telluride (fe) and of interstial iron defect (fd) in FeTe.

Composition supercell	a [Å]	c [Å]	$V/8$ [Å^3]	z_{Te}	z_{Feint}	(fe) [eV/atom]	(fd)
$Fe_{16}Te_{16}$	7.625	12.895	93.724	0.256		0.0223	
$Fe_{17}Te_{16}$	7.596	12.960	93.463	0.265	0.699	0.0565	1.13
$Fe_{16}Te_{15}Sb$	7.593	12.935	93.215	0.245		0.0435	0.68
$Fe_{15}NiTe_{16}$	7.644	12.862	93.956	0.245		0.0110	−0.59
$Fe_{15}CoTe_{16}$	7.633	12.883	93.820	0.246		0.0040	−0.36

Now, let us discuss about doping by Co, Ni and Sb. Here, we have considered only the case of the substitution on respectively the Fe and Te sites. Our calculations indicate that Ni doping and Co doping are much more favourable for stabilizing iron telluride than Sb doping that has more neutral effect. Therefore, in principle the Ni is the most stable dopant, agreeing with our experiments and with previous work in the literature studying Fe–Ni–Te phase diagram [16]. Note that the non trivial behaviour of the lattice parameter with Ni doping, i. e. the increase of the a lattice parameter and a decrease of the c lattice parameter with Ni doping, agree well with experimental observation for large Ni substitution by Rost and Akesson [16]. However, our calculations disagree with our experimental results concerning the Co doping. More experimental work is needed concerning that issue. Concerning the Sb doping, our stability calculations together with absence of change in the lattice parameter and the similarity ot the magnetic susceptibility of the Sb-doped sample with that one of $Fe_{1.13}Te$ indicates the possibility that the Sb doping was unsuccessful. Indeed, if the antimony was not entering in the FeTe structure, then the ratio Fe/Te is about 1.05 instead of 1 and it is therefore normal that the characteristics of the antimony doped sample are similar to that one of $Fe_{1.13}Te$.

The calculation of the electronic structure indicates that the main effect of I^{Fe} defect is to change the electronic structure around the Fermi level and to add some kinds of localized electronic level (see Fig. 2) and is not a doping effect, while Ni or Sb substitutions have only doping effect, the first one seems to give electron doping and the second one seems to give hole doping.

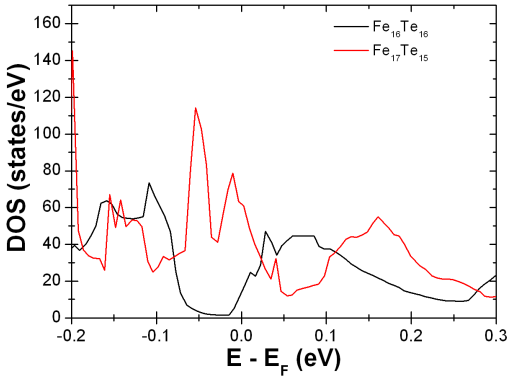

Fig. 2. Electronic density of states of $Fe_{16}Te_{16}$ supercell and $Fe_{17}Te_{16}$ supercell (corresponding to the case of I^{Fe} defect).

5. Conclusion

We were able to dope iron telluride only with Ni, while it was not possible with Co and some doubts remain about the success of antimony doping. Indeed, no change of lattice parameters and similar T_{trans} found in the antimony doped sample with the $Fe_{1.13}Te$. sample suggests that maybe only few antimony is entered in the lattice of iron telluride. The observation of lower stability of antimony doping compared to Co and Ni doping with structure relaxation calculations also agree with this picture. On the other hand, the stability calculations indicate that Ni doping is more favorable, in agreement with experiment. The Ni doping is found to be efficient to decrease the T_{trans} of the magnetic transition, opening an interesting way to combine Ni doping with pressure

or Se alloying for permitting the appearance of superconducting state. The calculations indicate that Ni or Sb substitutions have only doping effect, the first one seems to give electron doping and the second one seems to give hole doping. However, we note that more accurate calculations are needed to definitely conclude. Our first principles supercell calculations on defects stability confirm, for the first time, that the most stable defect in FeTe is the interstitial iron defect, confirming the current experimental view. In that case, electronic structure calculations indicate the appearance of large peak around the Fermi level that must affect strongly the magnetic and electronic properties of $Fe_{1+x}Te$ and its related alloys and could explain why they depend so much to iron content in the interstitial position. Giving the similarity of this large feature close to the Fermi level with resonance peak in Kondo effect, we can suggest that the highly localized electronic levels of these interstitial iron atoms can easily explain the Kondo-like behaviour observed in numerous physical properties of iron chalcogenides and notably the negative slope of the resistivity and Curie–Weiss behaviour in the magnetic susceptibility.

Acknowledgements

I would like to acknowledge E. Giannini and D. van der Marel and the support of the University of Geneva during my postdoctoral work for the large part of the experimental work, R. Cerny and F. Duc for the analysis of iron content from X-ray diffraction experiment, Ph. Jund for the use of his computing resources and helpful discussions about computing.

References

[1] K. Ishida, Y. Nakai, H. Hosono, *J. Phys. Soc. Jpn.* **78**, 062001, (2009).

[2] D.C. Johnston, *Adv. Phys.* **59**, 803, (2010).

[3] R. Viennois, E. Giannini, D. van der Marel, R. Cerny, *J. Solid State Chem.* **183**, 769, (2010).

[4] P.E. Blöchl, *Phys. Rev. B* **50**, 17953, (1994).

[5] G. Kresse, J. Furthmüller, *Phys. Rev. B* **54**, 11169, (1996).

[6] G. Kresse, D. Joubert, *Phys. Rev. B* **59**, 1758, (1999).

[7] J.P. Perdew, K. Burke, M. Ernzerhof, *Phys. Rev. Lett.* **77**, 3865, (1996).

[8] H.J. Monkhorst, J.D. Pack, *Phys. Rev. B* **13**, 5188, (1976).

[9] M. Methfessel, A.T. Paxton, *Phys. Rev. B* **40**, 3616, (1989).

[10] E.E. Rodriguez, C. Stock, P. Zajdel, K.L. Krycka, C.F. Majkrzak, P. Zavalij, M.A. Green, *Phys. Rev. B* **84**, 064403, (2011).

[11] I. Pallechi, G. Lamura, M. Tropeano, M. Putti, *Phys. Rev. B* **80**, 214511, (2009).

[12] H. Ipser, K.L. Komarek, H. Mikler, *Mh. Chem.* **105**, 1322, (1974).

[13] W. Schuster, H. Mikler, K.L. Komarek, *Mh. Chem.* **110**, 1153, (1979).

[14] J. Harl, G. Kresse, *Phys. Rev. Lett.* **103**, 056401, (2009).

[15] E. Pomjakushina, K. Conder, V. Pomjakushin, M. Bendele, R. Khasanov, *Phys. Rev. B* **80**, 024517, (2009).

[16] E. Rost, G. Akesson, *Acta Chem. Scand.* **26**, 3662, (1972).